Intrinsic magnetic properties of $R\mathrm{Fe}_{10}\mathrm{Mo}_2$ compounds (R = Y, Pr, Nd, Sm, Gd, Tb, Dy, Ho, Er, or Tm)

X. C. Kou, R. Grössinger, and G. Wiesinger
Institut für Experimentalphysik, Technische Universität Wien, Wiedner Hauptstraße 8-10, A-1040 Wien, Austria

J. P. Liu and F. R. de Boer
Van der Waals–Zeeman Laboratory, University of Amsterdam, Valckenierstraat 65-67, 1018 XE Amsterdam, The Netherlands

I. Kleinschroth and H. Kronmüller
Max Planck Institut für Metallforschung, Institut für Physik, Heisenbergstrasse 1, 70569 Stuttgart, Germany
(Received 9 May 1994)

A systematic investigation of the intrinsic magnetic properties of $R\mathrm{Fe}_{10}\mathrm{Mo}_2$ compounds (with R = Y, Pr, Nd, Sm, Gd, Tb, Dy, Ho, Er, and Tm) has been performed by means of ac susceptibility measurements, singular-point-detection techniques, and magnetization measurements. Spin reorientations were detected by measuring the temperature dependence of the ac susceptibility and the magnetization in $\mathrm{NdFe}_{10}\mathrm{Mo}_2$ (T_{sr} = 147 K), $\mathrm{DyFe}_{10}\mathrm{Mo}_2$ (T_{sr} = 137 K), $\mathrm{ErFe}_{10}\mathrm{Mo}_2$ (T_{sr} = 180 K), and $\mathrm{TmFe}_{10}\mathrm{Mo}_2$ (T_{sr} = 166 K). In order to trace field-induced magnetic phase transitions, magnetization curves were measured at 4.2 K on magnetically-aligned $R\mathrm{Fe}_{10}\mathrm{Mo}_2$ samples in magnetic fields up to 35 T in the Amsterdam high field installation. First-order magnetization processes (FOMP)-like transitions were detected at 4.2 K in $\mathrm{PrFe}_{10}\mathrm{Mo}_2$ (B_{cr} = 5.97 T) and $\mathrm{HoFe}_{10}\mathrm{Mo}_2$ (B_{cr} = 1.73 T) in an external field applied perpendicular to the alignment direction and in $\mathrm{ErFe}_{10}\mathrm{Mo}_2$ (B_{cr} = 2.47 T) in an external field applied parallel to the alignment direction. An anomalous increase of magnetization of $\mathrm{SmFe}_{10}\mathrm{Mo}_2$ at low temperatures in an external field applied perpendicular to the alignment direction is suggested to be due to a fast continuous rotation of magnetic moment under the action of external field, rather than due to a FOMP-type transition. The magnetic-coupling strength between the rare-earth and the transition-metal moments have been determined for the $R\mathrm{Fe}_{10}\mathrm{Mo}_2$ compounds with R = Dy, Ho, Er, or Tm from the magnetization behavior in fields up to 35 T of fine single-crystalline powder particles, loaded loosely into the sample holder and therefore free to rotate in the applied magnetic field. The temperature dependence of the anisotropy field B_A of the $R\mathrm{Fe}_{10}\mathrm{Mo}_2$ compounds has been determined by means of the singular-point-detection technique in the temperature interval where the easy magnetization direction of the samples is parallel to the c axis. It is found that an annealing treatment of the as-cast ingots of the $R\mathrm{Fe}_{10}\mathrm{Mo}_2$ compounds at high temperature (at least 1323 K) for a long time (at least two weeks) is vital to obtain $R\mathrm{Fe}_{10}\mathrm{Mo}_2$ compounds with the tetragonal ThMn_{12} structure.

I. INTRODUCTION

In searching for Fe-rich rare-earth (R) intermetallic compounds suitable for permanent-magnet fabrication, the tetragonal $R(\mathrm{Fe},M)_{12}$ compounds (M = Ti, Si, V, Cr, Mo, or W) have shown to be worth investigating further.[1–5] Some common features of these compound series can be summarized as follows: (1) There is only one crystallographic rare-earth site which simplifies the study of the crystalline electric field (CEF) effect on the rare-earth ion in these compounds.[6–8] (2) Pure $R\mathrm{Fe}_{12}$ compounds with the tetragonal ThMn_{12} structure (space group $I4/mmm$) are not stable for all R elements. The M atoms in $R(\mathrm{Fe},M)_{12}$, which preferentially occupy one of the three Fe sites $8f$, $8i$, or $8j$ stabilize the structure. In most cases, the M atoms occupy the $8i$ site.[9,10] (3) The magnetic anisotropy of the Fe sublattice favors the c axis. (4) Only Sm-containing compounds show the high uniaxial anisotropy field which is of vital importance in establishing the coercivity of a possible magnet. However, the coercivity realized thus far is disappointing.[11,12] (5) The contribution from the R sublattice to the anisotropy is not completely predictable from the second-order CEF term only. This suggests that fourth-order as well as sixth-order CEF terms play an important role in determining the easy magnetization direction (EMD). From the CEF calculations, it follows that fourth- or sixth-order CEF terms lead to an EMD that deviates from the c axis. Therefore field- and temperature-induced magnetic phase transitions, like first-order magnetization processes and spin reorientations, may be expected to occur in $R(\mathrm{Fe},M)_{12}$-type compounds. Among the $R(\mathrm{Fe},M)_{12}$ compounds, the $R\mathrm{Fe}_{10}\mathrm{Mo}_2$ series is anomalous in several respects. First of all, the $R\mathrm{Fe}_{10}\mathrm{Mo}_2$ compounds have the lowest Curie temperatures and the lowest magnetization of all corresponding $R(\mathrm{Fe},M)_{12}$ compounds.[13] Furthermore, some magnetic anomalies, like a spin-glass-like transition, have been reported in $\mathrm{YFe}_{10}\mathrm{Mo}_2$ and $\mathrm{LuFe}_{10}\mathrm{Mo}_2$.[13,14] Very recently, Sun *et al.*[15,16] have reported that $\mathrm{YFe}_{12-x}\mathrm{Mo}_x$ compounds can be stabilized in the tetragonal ThMn_{12} structure with x as low as 0.5. The magnetization and Curie temperatures of

$YFe_{12-x}Mo_x$ increase markedly with decreasing Mo concentration. In addition, it has been found that $SmFe_{11.5}Mo_{0.5}$ exhibits an anisotropy field as high as 10 T at room temperature.[17] All these facts make the $RFe_{12-x}Mo_x$ compounds interesting from both technical and fundamental points of view. In the present study, we report a systematic experimental investigation of the $RFe_{10}Mo_2$ series. The main emphasis has been given to the magnetocrystalline anisotropy and to magnetic phase transitions. The study of the intersublattice exchange interaction between the R and T sublattice is another important point in the present study.

The present paper is organized as follows: The experimental procedures are described in detail in Sec. II. In Sec. III, the fundamental background of the magnetic phase transition and the magnetic exchange interaction in the R-T intermetallic compounds is reviewed. The experimental results are presented and discussed in Sec. IV. Finally, in Sec. V, a summary and some general conclusions are presented.

II. EXPERIMENTAL DETAILS

Polycrystalline $RFe_{10}Mo_2$ ingots with R = Y, Pr, Nd, Sm, Gd, Tb, Dy, Ho, Er, and Tm were prepared by induction melting appropriate amounts of the starting materials of a purity of at least of 99.99 wt. %. The ingots were remelted four times in order to achieve homogeneity. Weight losses during the melting due to evaporation of the rare-earth element were compensated for by starting with an excess of 3 wt. % R (with respect to the R content). The as-cast ingots were wrapped in tantalum foil and sealed in a preevacuated and then argon-gas-filled quartz tube, followed by annealing at 1373 K for 4 weeks. In order to avoid possible crystallographic phase transitions during the cooling process, the samples were quenched in water. It was found that the annealing treatment of the as-cast ingots was necessary to obtain tetragonal $RFe_{10}Mo_2$ compounds. The $RFe_{10}Mo_2$ compounds with $ThMn_{12}$ tetragonal structure could only be obtained through an annealing process at high temperature (at least 1323 K) for a long time (at least 2 weeks).[18] The purity of samples was checked by x-ray diffraction, using Cr $K\alpha$ radiation, and by optical microscopy. It was found that after the above annealing treatment all investigated samples were single phase with the desired tetragonal $ThMn_{12}$ structure. The occupation by Mo atoms of the three possible Fe sites 8f, 8i, and 8j was determined by analyzing the x-ray-diffraction patterns. The Mo atoms were found to occupy only 8i sites.[10] For this reason, well-annealed $RFe_{10}Mo_2$ can be considered as true ternary compounds. The lattice constants a and c derived from the x-ray-diffraction analysis are listed in Table I. Magnetically aligned samples with a cylindrical shape were prepared by aligning at room temperature fine particles with a diameter smaller than 40 μm (obtained by powdering by hand in a mortar) parallel and perpendicular to the cylinder axes in a magnetic field of 1 T and by fixing their direction with epoxy resin. The temperature dependence of the magnetization of the $RFe_{10}Mo_2$ compounds was measured in a low applied field (0.05 T) in a vibrating-sample magnetometer (VSM) equipped with a superconducting coil. This equipment can be operated in a temperature range from 4.2 to 800 K. The Curie temperatures of the $RFe_{10}Mo_2$ compounds obtained in these measurements are also listed in Table I. The temperature dependence of the ac susceptibility of the $RFe_{10}Mo_2$ compounds was measured in a susceptometer which can be operated from 1.8 to 300 K with ac fields up to 0.001 T and frequencies from 5 to 1000 Hz. The temperature dependence of the anisotropy field B_A was determined by means of the singular-point-detection (SPD) technique in a pulsed-field magnetometer which can be operated from 4.2 to 1000 K with a maximum field of 30 T. The magnetization at 4.2 K of magnetically aligned $RFe_{10}Mo_2$ compounds was measured with the field applied parallel or

TABLE I. Magnetic properties of $RFe_{10}Mo_2$ compounds. a and c are the lattice constants. T_c and T_{SR} are the Curie temperature and the spin-reorientation temperature, respectively. M_S is the spontaneous magnetization expressed in μ_B/f.u. M_R is the saturation moment of the free R^{3+} ion (in μ_B/atom). M_T is the magnetic moment of the transition-metal sublattice, expressed in μ_B/f.u. B_A and B_{cr} are the anisotropy field and the critical field of the FOMP, respectively.

Compound	a (nm) (300 K)	c (nm) (300 K)	T_c (K)	T_{SR} (K)	M_S (4.2 K)	M_R	M_T (4.2 K)	B_A (T) (4.2 K)	B_{cr} (T) (4.2 K)
$YFe_{10}Mo_2$	0.8554	0.4798	317		14.06	0	14.06	1.27	
$PrFe_{10}Mo_2$	0.8624	0.4804	365		17.65	3.20	14.45		5.97
$NdFe_{10}Mo_2$	0.8613	0.4805	366	147	18.22	3.27	14.95		
$SmFe_{10}Mo_2$	0.8582	0.4795	429		18.44	0.71	17.73	4.77[a]	7.15[b]
$GdFe_{10}Mo_2$	0.8571	0.4802	444			7		3.24	
$TbFe_{10}Mo_2$	0.8558	0.4799	360		6.15	9	15.15		
$DyFe_{10}Mo_2$	0.8543	0.4791	335	137	5.52	10	15.52	0.43[a]	
$HoFe_{10}Mo_2$	0.8534	0.4789	310		4.91	10	14.91		1.73
$ErFe_{10}Mo_2$	0.8527	0.4786	289	180	5.96	9	14.96		2.61
$TmFe_{10}Mo_2$	0.8516	0.4783	261	166	6.70	7	13.70		

[a]Values at 300 K.
[b]Value of B_S.

perpendicular to the alignment direction in fields up to 35 T in the Amsterdam High Field Installation.[19] In order to determine the magnetic-coupling strength between the R and T moments, high-field magnetization measurements were performed on fine (single-crystalline) powder particles loaded loosely into a sample holder and therefore free to rotate in the applied magnetic field. These experiments have been done on $R\mathrm{Fe}_{10}\mathrm{Mo}_2$ compounds where R is one of the heavy rare-earth elements Tb, Dy, Ho, Er, or Tm.

III. FUNDAMENTAL BACKGROUND OF THE MAGNETIC PHASE TRANSITION AND EXCHANGE INTERACTION IN THE R-T INTERMETALLIC COMPOUNDS

In R-T compounds, the contribution to the anisotropy from the R sublattice generally dominates at low temperatures, whereas the T-sublattice anisotropy dominates at high temperatures. Also, the R-sublattice anisotropy decreases much faster with temperature than the T-sublattice anisotropy. In $R\mathrm{Fe}_{10}\mathrm{Mo}_2$ compounds, the Fe-sublattice anisotropy favors the c axis,[20] whereas the R-sublattice anisotropy depends on the CEF interaction and the exchange field experienced by R ions. If one considers only the second-order CEF term, the Sm, Er, and Tm sublattices in $R\mathrm{Fe}_{10}\mathrm{Mo}_2$ should have a c-axis contribution to the net anisotropy, whereas the remaining magnetic R ions should have planar contributions to the net anisotropy. Therefore many spin-reorientation transitions, temperature-induced changes of the EMD, are expected in $R\mathrm{Fe}_{10}\mathrm{Mo}_2$, either due to the temperature-induced competition between the R- and Fe-sublattice anisotropies or due to temperature-induced changes in the R sublattice only. Another magnetic phase transition which often takes place in R-T intermetallics is the first-order magnetization process (FOMP). A FOMP manifests itself as a discontinuous change of the magnetization measured with the field applied parallel to a specific crystallographic direction and is characterized by a critical temperature T_{FOMP}, below which the FOMP occurs,[21] and by a critical field B_{cr}. The physical origin of the FOMP is that two relative minima appear in the total energy (as a function of the angle between a particular crystallographic direction and the magnetization) and compete with each other according to temperature and the strength of applied magnetic field.

The indirect exchange interaction between the $3d$ spins of the T metal and the $4f$ spins of the R elements couples the moments of the light (less than half-full $4f$ shell) R elements parallel (ferromagnetically) to the T moments, whereas the moments of the heavy (more than half-full $4f$ shell) R elements will be oriented antiparallel (ferrimagnetically) with respect to the T moments. The magnetic properties, e.g., the magnetic anisotropy, the magnetization, etc., depend to a large extent on the strength of the R-T exchange interaction. One way to obtain information on the R-T interaction is by comparing the Curie temperatures of compounds containing magnetic and nonmagnetic R atoms (Y, La, and Lu) and obtaining the intersublattice-interaction molecular-field coefficient $n_{R\text{-}T}$ by analyzing the Curie temperatures in a molecular-field description (see, e.g., Refs. 22 and 23). For Gd-containing compounds, the value of the exchange field at the Gd sites can be directly determined by inelastic neutron scattering.[24] For ferrimagnetic materials, $n_{R\text{-}T}$ can be determined in a very elegant and direct way from the magnetization in high magnetic fields. This method was first developed for garnets without taking into account the magnetocrystalline anisotropy.[25] Grössinger and Hilscher [26] have tried to use this method to analyze the intersublattice exchange of $\mathrm{Er}_6\mathrm{Fe}_{23}$ and to include the anisotropy energy by taking into account the anisotropy constants up to the fourth order.[27] Recently, Verhoef, Radwanski, and Franse[28] have developed a method for ferrimagnetic R-T compounds with very large R-sublattice anisotropy and negligible T-sublattice anisotropy. They allowed fine single-crystalline particles to rotate freely in the applied magnetic field and studied the magnetization process in the field region where the magnetic configuration deviates from the exact ferrimagnetic configuration. By this method, a large variety of ferrimagnetic R-T compounds has been investigated in recent years in the Amsterdam High Field Installation. A comprehensive review of this work has been given by Liu *et al.*[29] The interpretation of the experimental results is based on a molecular-field description.[25,28,30] In a ferrimagnetic compound, the phenomenological expression for the total energy E_t is

$$E_t = E_a + n_{R\text{-}T} M_R M_T \cos\alpha - B\sqrt{M_R^2 + M_T^2 + 2M_R M_T \cos\alpha}\ , \tag{1}$$

where $E_a = E_{aT} + E_{aR}$ is the total anisotropy energy with E_{aT} the T-sublattice anisotropy energy and E_{aR} the R-sublattice anisotropy energy. M_R, M_T, α, B, and $n_{R\text{-}T}$ are the R-sublattice moment, the T-sublattice moment, the angle between M_R and M_T, the applied field, and the intersublattice-molecular-field coefficient, respectively. The equilibrium state of M_R and M_T can be obtained by minimizing Eq. (1) with respect to α,

$$\frac{\partial E_t}{\partial \alpha} = \frac{\partial E_a}{\partial \alpha} - n_{R\text{-}T} M_R M_T \sin\alpha + \frac{B M_R M_T \sin\alpha}{\sqrt{M_R^2 + M_T^2 + 2M_R M_T \cos\alpha}} \tag{2a}$$

and

$$\frac{\partial E_t}{\partial \alpha} = 0\ . \tag{2b}$$

The simplest case for which $\partial E_t/\partial\alpha = 0$ is $\partial E_a/\partial\alpha = 0$, which requires, in the case that the single crystal is fixed with respect to the field direction, $\partial E_{aR}/\partial\alpha = 0$ and $\partial E_{aT}/\partial\alpha = 0$; i.e., both E_{aT} and E_{aR} should be constant with respect to α. If the single crystal is allowed to orient itself with respect to the field direction, the two cases—either E_{aT} or E_{aR} is constant with respect to α—lead to the condition $\partial E_t/\partial\alpha = 0$. It is worth noting that the condition $\partial E_t/\partial\alpha = 0$ cannot be satisfied even if the single crystal is allowed to rotate freely in applied magnetic

fields if both E_{aT} and E_{aR} are not constant with respect to α. However, for R-T compounds, E_{aT} is, in most cases, at least one order of magnitude smaller than E_{aR} at low temperatures. Therefore, in most cases, the T-sublattice anisotropy can be neglected. If $\partial E_t/\partial\alpha=0$, two equilibrium states can be determined by solving Eq. (2b);

$$\text{(I)}\quad \sin\alpha=0\ , \tag{3}$$

which corresponds with $\alpha=0°$ or 180°, i.e., M_T and M_R either parallel (high fields) or antiparallel (low fields), and

$$\text{(II)}\quad \cos\alpha=\frac{(B/n_{R\text{-}T})^2-M_R^2-M_T^2}{2M_RM_T}\ . \tag{4}$$

In this case, since $-1\le\cos\alpha\le 1$, two critical fields B_1 and B_2 can be obtained:

$$B_1=n_{R\text{-}T}|M_R-M_T|\ , \tag{5}$$

below which M_R is perfectly antiparallel to M_T, and

$$B_2=n_{R\text{-}T}(M_R+M_T)\ , \tag{6}$$

above which M_R is exactly parallel to M_T. In the intermediate-field range between B_1 and B_2, one obtains

$$M=\frac{B}{n_{R\text{-}T}}\ , \tag{7}$$

with M, the measured magnetization, given by

$$M^2=M_R^2+M_T^2+2M_RM_T\cos\alpha\ . \tag{8}$$

In the intermediate-field range, the magnetization depends linearly on the field with a slope $1/n_{R\text{-}T}$. The above description is illustrated in Fig. 1.[31] In the present paper, we have applied this method to determine $n_{R\text{-}T}$ for the RFe$_{10}$Mo$_2$ compounds with R=Dy, Ho, Er, and Tm. However, one should keep in mind that the Fe-sublattice anisotropy is neglected in the analysis presented above. A more complex, therefore more general, calculation for R-T compounds taking into account the 3d-sublattice anisotropy has been carried out by Zhao.[32] A more extended analysis of the free-powder magnetization results for RFe$_{10}$Mo$_2$ compounds with R=Dy, Ho, Er, and Tm, taking into account the Fe-sublattice anisotropy, will be published elsewhere.[33]

In order to make it possible to compare the intersublattice-magnetic-coupling strengths in various R-T compounds, one may convert $n_{R\text{-}T}$ to the intersublattice exchange constant $J_{R\text{-}T}$ that is independent of the number $Z_{R\text{-}T}$ of T neighbors surrounding the R atoms and that is expressed per (unit moment)^2 of a pair of R and T atoms. $n_{R\text{-}T}$ is related to $J_{R\text{-}T}$ appearing in the interaction Hamiltonian $H_{\text{exch}}=\sum 2J_{R\text{-}T}\mathbf{S}_R\cdot\mathbf{S}_T$ via the expression[28]

$$n_{R\text{-}T}=-\frac{J_{R\text{-}T}Z_{R\text{-}T}(g_R-1)}{N_T\mu_B^2g_R}\ , \tag{9}$$

where $Z_{R\text{-}T}$ is the number of nearest T neighbors to an R atom ($Z_{R\text{-}T}$=20 in RFe$_{10}$Mo$_2$), N_T is the number of T atoms per formula unit (N_T=12 for RFe$_{10}$Mo$_2$), and g_R is the Landé factor of the R^{3+} ion, which is listed in Table II.

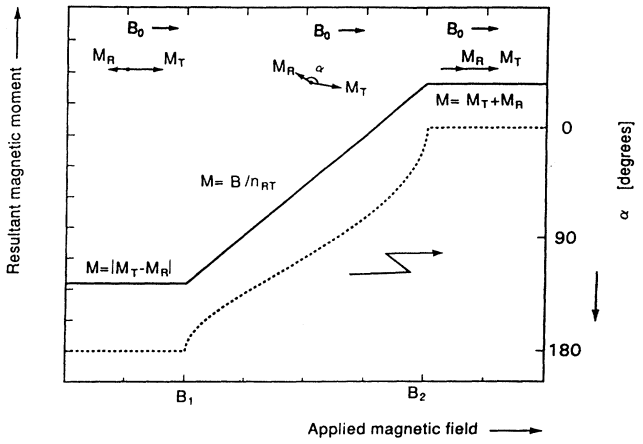

FIG. 1. Resultant magnetic moment of a free ferrimagnetic R-T single crystal with zero T-sublattice anisotropy. The dashed line gives the angle between the two magnetization vectors (after Ref. 31).

IV. EXPERIMENTAL RESULTS AND DISCUSSION

A. YFe$_{10}$Mo$_2$ and GdFe$_{10}$Mo$_2$

The compounds YFe$_{10}$Mo$_2$ and GdFe$_{10}$Mo$_2$ can be expected to exhibit very similar magnetic anisotropy since Y is nonmagnetic and Gd is an S-state ion, so that these two compounds can be considered as pure "3d compounds," in which only the Fe sublattice contributes to the anisotropy. Both compounds have been reported to exhibit uniaxial anisotropy.[20]

TABLE II. Intersublattice-molecular-field coefficients $n_{R\text{-}T}$ in units of Tf.u./μ_B or Tm/A, the Landé factor g_R of R^{3+}. The density d of RFe$_{10}$Mo$_2$ is calculated from the lattice constants. Also given are the experimental first critical field $B_{1\,\text{expt}}$ and the R-T exchange constant $J_{R\text{-}T}$ of RFe$_{10}$Mo$_2$ compounds with R representing Dy, Ho, Er, and Tm.

Compounds	$n_{R\text{-}T}$ (Tf.u./μ_B)	$n_{R\text{-}T}$ (Tm/A)	g_R	d (g/cm^3)	$B_{1\,\text{expt}}$ (T)	$-J_{R\text{-}T}/k$ (K)
DyFe$_{10}$Mo$_2$	5.74	8.13×10^{-3}	$\frac{4}{3}$	8.67	28.1	9.3
HoFe$_{10}$Mo$_2$	3.73	5.33×10^{-3}	$\frac{5}{4}$	8.72	20.0	6.9
ErFe$_{10}$Mo$_2$	2.38	3.42×10^{-3}	$\frac{6}{5}$	8.76	16.7	5.4
TmFe$_{10}$Mo$_2$	2.72	3.95×10^{-3}	$\frac{7}{6}$	8.80	15.8	5.7

The temperature dependence of the ac susceptibility of $YFe_{10}Mo_2$ and $GdFe_{10}Mo_2$ has been measured from 4.2 to 300 K. No anomaly was detected, suggesting that the EMD of the Fe-sublattice magnetization is parallel to the c axis in this temperature range. Figure 2 shows the temperature dependence of the anisotropy field B_A of the two compounds determined with the SPD technique. The second-order anisotropy constant K_1 can be obtained by $K_1=0.5M_SB_A$. It is noted that the anisotropy in $YFe_{10}Mo_2$ reflects directly the Fe-sublattice anisotropy of the $RFe_{10}Mo_2$ compounds. However, possibly because of a noncollinear configuration of the Fe and Gd moments in an external field, the anisotropy field of $GdFe_{10}Mo_2$ shows a deviation. It is noted that such a deviation is only pronounced in $GdCo_5$ compounds[34–36] and exists very slightly in, e.g., $Gd_2Fe_{14}B$,[37,38] $GdFe_{11}Ti$,[8] and Gd_2Fe_{17}.[39]

Compared to $YFe_{11}Ti$ and $GdFe_{11}Ti$,[8] the values of B_A of $YFe_{10}Mo_2$ and $GdFe_{10}Mo_2$ are rather small. The SPD measurement confirms that the EMD in $GdFe_{10}Mo_2$ is parallel to the c axis in the whole temperature range of magnetic ordering. However, in $YFe_{10}Mo_2$ the anisotropy field is detectable only below 150 K, much lower than the Curie temperature of 317 K. A similar phenomenon was reported by Christides *et al.*[13,14] who proposed a spin-glass-like transition. In fact, as shown in Fig. 3, an anomaly in the temperature dependence of the magnetization of $YFe_{10}Mo_2$ does appear around 150 K. We are not able to provide an explanation for this anomaly. The high-field magnetization of $YFe_{10}Mo_2$ at 4.2 K confirms the uniaxial anisotropy (Fig. 4). The value of the spontaneous magnetization M_S of $YFe_{10}Mo_2$ obtained by linear extrapolation of the high-field (above 8 T) magnetization to $B=0$ is listed in Table I. From M_S, the mean Fe moment at 4.2 K was deduced to be $1.4\mu_B$/Fe. This is very small compared to other $Y(Fe,M)_{12}$ compounds, for instance, $1.7\mu_B$/Fe atom in $YFe_{11}Ti$.[8] The small values of M_S and B_A for $YFe_{10}Mo_2$ lead to the conclusion that the Fe-sublattice anisotropy energy

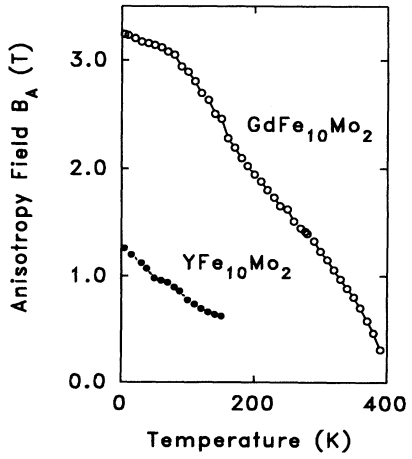

FIG. 2. Temperature dependence of the anisotropy field B_A of $YFe_{10}Mo_2$ (●) and $GdFe_{10}Mo_2$ (○) determined by the SPD technique.

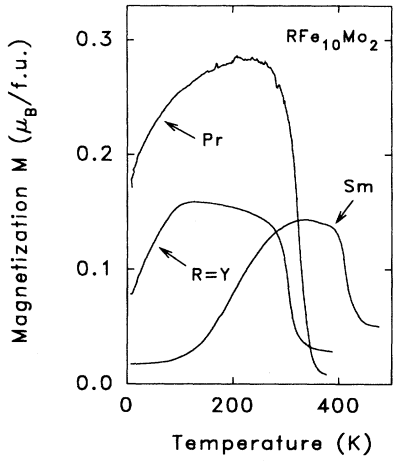

FIG. 3. Temperature dependence of the magnetization of $RFe_{10}Mo_2$ with R = Y, Pr, and Sm in an external field of 0.05 T.

($K_1=0.5B_AM_S$) is small in $RFe_{10}Mo_2$ compounds. The low values of M_S and also of T_C for $YFe_{10}Mo_2$ may be due to the reduction of the interatomic Fe-Fe distance.[40]

B. $PrFe_{10}Mo_2$

Because of difficulties in preparing $PrFe_{10}Mo_2$ with the tetragonal $ThMn_{12}$ structure, there exists, to our knowledge, no previous report on this compound. In the present study, single-phase $PrFe_{10}Mo_2$ was obtained by annealing as-cast $PrFe_{10}Mo_2$ ingots at high temperature (1373 K) for a long time (4 weeks). Because of the large planar Pr-sublattice anisotropy in $Pr(Fe,M)_{12}$ compounds,[8] the EMD of $PrFe_{10}Mo_2$ is expected to be of basal-plane type at low temperatures. The temperature dependence of the ac susceptibility (Fig. 5) and of the magnetization (Fig. 3) does not reveal any anomaly up to the Curie temperature, implying that the planar Pr-sublattice anisotropy is stronger than the uniaxial Fe-sublattice anisotropy over the whole temperature range of magnetic ordering.

Magnetization measurements performed on magnetically aligned $PrFe_{10}Mo_2$ at 4.2 K in fields applied parallel

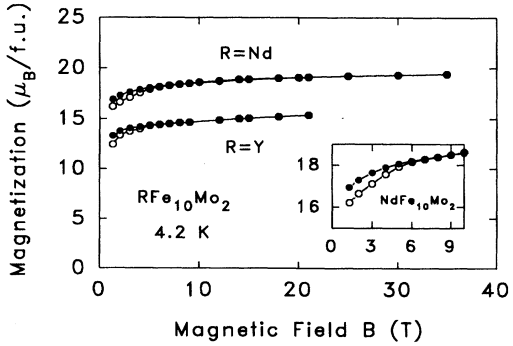

FIG. 4. High-field magnetization at 4.2 K of magnetically aligned $YFe_{10}Mo_2$ and $NdFe_{10}Mo_2$ with the field applied parallel (●) and perpendicular (○) to the alignment direction.

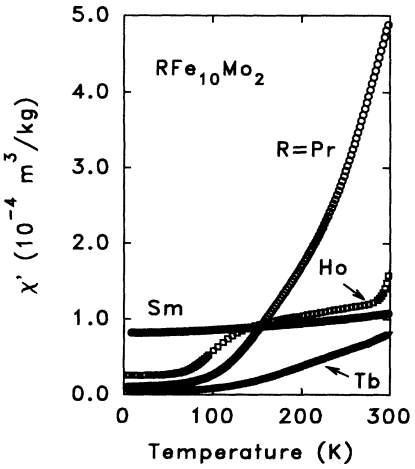

FIG. 5. Temperature dependence of the real component χ' of the ac susceptibility of RFe$_{10}$Mo$_2$ compounds with R = Pr, Sm, Tb, and Ho. The applied ac field was 5×10^{-5} T and the frequency 1000 Hz.

and perpendicular to the alignment direction are shown in Fig. 6. An anomalous increase of the magnetization is found when the external field is applied perpendicular to the alignment direction. As discussed above, the EMD in PrFe$_{10}$Mo$_2$ is in the basal plane over the whole temperature range of magnetic ordering. The magnetic alignment at room temperature ensures that the c axis is within the plane perpendicular to the alignment direction. Therefore the anomaly observed when the external field is perpendicular to the alignment direction can be attributed to a FOMP-like transition occurring when the external field is applied parallel to the c axis. The value of the critical field B_{cr} of this FOMP-type transition can be determined from the maximum of the dM/dB versus B curve.[8,21,41] From the shape of this curve, further information concerning the FOMP transition can be deduced.[41] In addition, it is interesting that PrFe$_{10}$Mo$_2$ is the only Pr-containing tetragonal ThMn$_{12}$ type of compound that shows a FOMP-like transition at low temperatures. It is suggested that this FOMP-like transition is due to the higher-order CEF terms of the Pr ion.

C. NdFe$_{10}$Mo$_2$

Figure 7 shows the temperature dependence of the ac susceptibility of NdFe$_{10}$Mo$_2$. Like in NdFe$_{11}$Ti,[6,8] a peaklike anomaly, indicating a spin-reorientation transition, is found at about 147 K. The temperature dependence of the magnetization of NdFe$_{10}$Mo$_2$ in the temperature range from 4.2 K to the Curie temperature shows that this is the only spin reorientation detectable below the magnetic-ordering temperature (Fig. 8). At room temperature, the anisotropy field of NdFe$_{10}$Mo$_2$ as detected by the SPD technique is fairly small. This leads to a bad magnetic alignment of the NdFe$_{10}$Mo$_2$ powder, which clearly can be seen (Fig. 4) in the magnetization of magnetically aligned NdFe$_{10}$Mo$_2$ with the field applied parallel to perpendicular to the alignment direction. Concerning the magnetization at 4.2 K of powders of polycrystalline materials that have magnetically been aligned at room temperature, three cases can be distinguished: (1) No change of the EMD occurs. In this case, the low-field susceptibility measured with the field applied parallel to the alignment direction is much lower (near zero) than that measured with the field applied perpendicular to the alignment direction in the ranges of both the fields up to the anisotropy field B_A. (2) The EMD changes from the c axis (room temperature) to a cone (4.2 K). In this case, the values of the susceptibility measured with field applied parallel or perpendicular to the alignment direction are large and of comparable value. If the values of the susceptibility measured with the field parallel to the alignment direction are larger than those measured with field perpendicular to the alignment direction, the cone angle at 4.2 K is larger than 45° and vice versa. (3) The EMD changes from the c axis (room temperature) to the basal plane (4.2 K). This is the

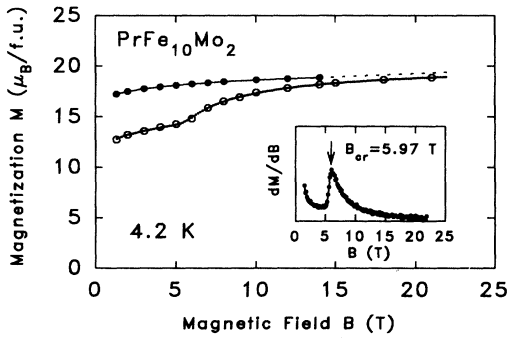

FIG. 6. High-field magnetization at 4.2 K of magnetically aligned PrFe$_{10}$Mo$_2$ with the field applied parallel (●) and perpendicular (○) to the alignment direction. The large and small dots represent the measurements obtained by employing "stepwise" and continuous" field pulses, respectively. The inset shows dM/dB vs B for determining the critical field B_{cr} of the FOMP.

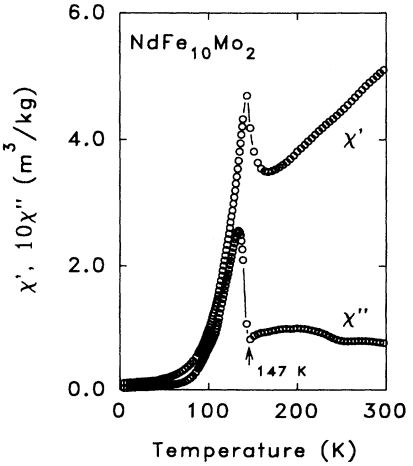

FIG. 7. Temperature dependence of the real (χ') and imaginary (χ'') components of the ac susceptibility of NdFe$_{10}$Mo$_2$. The applied ac field was 5×10^{-5} T and the frequency 1000 Hz.

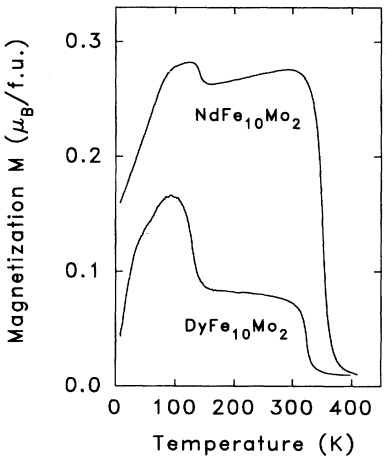

FIG. 8. Temperature dependence of the magnetization of $R\mathrm{Fe}_{10}\mathrm{Mo}_2$ compounds with R = Nd and Dy in an external field of 0.05 T.

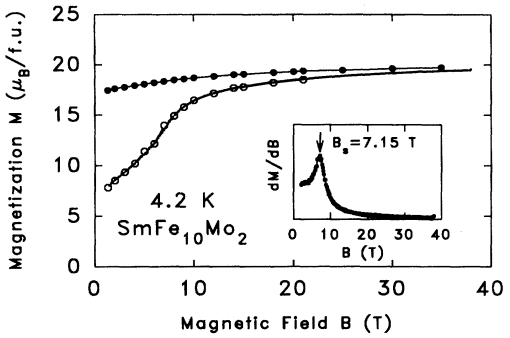

FIG. 9. High-field magnetization at 4.2 K of magnetically aligned $\mathrm{SmFe}_{10}\mathrm{Mo}_2$ with the field applied parallel (●) and perpendicular (○) to the alignment direction. The large and small dots represent the measurements obtained by employing "stepwise" and "continuous" field pulses, respectively. The inset shows dM/dB vs B for determining the critical field B_S.

reverse case of (1). According to these considerations, the magnetization of the magnetically aligned $\mathrm{NdFe}_{10}\mathrm{Mo}_2$ samples leads to the conclusion that the spin reorientation occurring in $\mathrm{NdFe}_{10}\mathrm{Mo}_2$ corresponds to a change of the EMD from the c axis ($T > 147$ K) to a cone ($T < 147$ K). Similar to what has been found in $\mathrm{NdFe}_{11}\mathrm{Ti}$,[8] the spin reorientation detected in $\mathrm{NdFe}_{10}\mathrm{Mo}_2$ is likely to be due to a temperature-induced competition among the different CEF terms of the Nd ion.

D. $\mathrm{SmFe}_{10}\mathrm{Mo}_2$

A FOMP-like transition in $\mathrm{SmFe}_{10}\mathrm{Mo}_2$ at low temperatures has been reported earlier.[20] The magnetic anisotropy of $\mathrm{SmFe}_{10}\mathrm{Mo}_2$, which is the largest of all $R\mathrm{Fe}_{10}$,Mo_2 compounds, is mainly due to the large uniaxial anisotropy of the Sm ions which ensures that the EMD of $\mathrm{SmFe}_{10}\mathrm{Mo}_2$ is parallel to the c axis at low temperature. The temperature dependence of the ac susceptibility (Fig. 5) and of the magnetization (Fig. 3) of $\mathrm{SmFe}_{10}\mathrm{Mo}_2$ give no evidence of a change of the EMD up to the Curie temperature. The magnetization of magnetically aligned $\mathrm{SmFe}_{10}\mathrm{Mo}_2$ samples was measured at 4.2 K with the field parallel and perpendicular to the alignment direction (Fig. 9). An anomalous increase of the magnetization is observed when the field is applied perpendicular to the alignment direction. The field B_S where the magnetization changes most rapidly is determined by the maximum in the dM/dB versus B curve (inset of Fig. 9). Such an "anomalous increase" of the magnetization at low temperatures is a common feature of Sm-containing ThMn_{12} type of compounds.[4,6,8,17,42] However, there are many different suggestions concerning the physical origin of this transition.[8] For $\mathrm{SmFe}_{11}\mathrm{Ti}$, measurements on single crystals[42] have shown that the anomalous increase found in the magnetization curve when an external field is applied perpendicular to the c axis is not a FOMP, but a fast continuous rotation of the magnetic moment under the action of the external field. For $\mathrm{SmFe}_{10}\mathrm{Mo}_2$, the same behavior as in $\mathrm{SmFe}_{11}\mathrm{Ti}$ may be expected.

The difference in the dM/dB versus B curves for $\mathrm{SmFe}_{10}\mathrm{Mo}_2$ (inset of Fig. 9), $\mathrm{PrFe}_{10}\mathrm{Mo}_2$ (inset of Fig. 6), $\mathrm{HoFe}_{10}\mathrm{Mo}_2$ (inset of Fig. 16), and $\mathrm{ErFe}_{10}\mathrm{Mo}_2$ (inset of Fig. 18) is evident. However, the details of the physical origin of the anomaly found in $\mathrm{SmFe}_{10}\mathrm{Mo}_2$ cannot be provided until magnetization measurements on a single crystal of $\mathrm{SmFe}_{10}\mathrm{Mo}_2$ are available. The temperature dependence of the anisotropy field B_A and of B_S of $\mathrm{SmFe}_{10}\mathrm{Mo}_2$ has been determined by the SPD technique (Fig. 10). From these measurements, it follows that the onset of this anomalous increase of magnetization of $\mathrm{SmFe}_{10}\mathrm{Mo}_2$ is at about 150 K.

E. $\mathrm{TbFe}_{10}\mathrm{Mo}_2$

In $\mathrm{TbFe}_{11}\mathrm{Ti}$ and $\mathrm{TbFe}_{10}\mathrm{V}_2$, spin-reorientation transitions have been detected.[8,43] The temperature dependence of the ac susceptibility of $\mathrm{TbFe}_{10}\mathrm{Mo}_2$ shows no indication

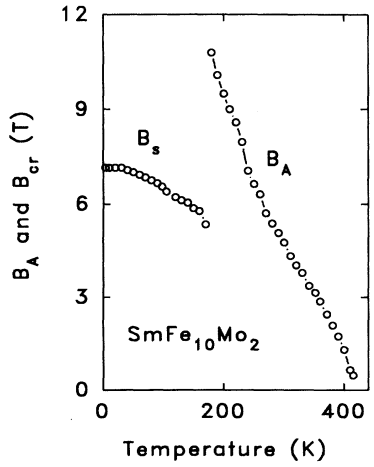

FIG. 10. Temperature dependence of the anisotropy field B_A and of B_S of $\mathrm{SmFe}_{10}\mathrm{Mo}_2$.

of a change of the EMD in the temperature interval from 4.2 to 300 K (Fig. 5). However, because of the basal plane of anisotropy of the Tb sublattice, one would expect a spin-reorientation transition at higher temperature, caused by the competition between the uniaxial Fe-sublattice anisotropy (less temperature dependent) and the Tb-sublattice anisotropy (more temperature dependent). In order to detect this possible spin-reorientation transition, the temperature dependence of the magnetization of TbFe$_{10}$Mo$_2$ was also measured (Fig. 11). However, no indication of a spin reorientation was found. This may be understood to be a consequence of a too small uniaxial Fe-sublattice anisotropy (see Sec. IV A) to compete with the planar Tb-sublattice anisotropy, which suggests that the EMD in TbFe$_{10}$Mo$_2$ is in the basal plane at all temperatures below the magnetic ordering temperature.

Figure 11 shows, with TbFe$_{10}$Mo$_2$ as an example, the importance of the annealing process in obtaining the tetragonal ThMn$_{12}$-type RFe$_{10}$Mo$_2$ compounds. One of the samples (a) was annealed at 1373 K for 2 weeks and other (b) for 4 weeks. The experimental result on the latter sample suggests that this sample has obtained the desired homogeneous ThMn$_{12}$ phase. The less-annealed sample is a mixture of TbFe$_{12-x}$Mo$_x$ with various x. It should be stated that it is a common feature of all the RFe$_{10}$Mo$_2$ samples studied that the ThMn$_{12}$ structure can only be obtained by annealing at high temperature for a long time. It is interesting that no large differences are detected in the x-ray-diffraction patterns of these two samples. In addition, a rather broad homogeneity range is proposed in R-Fe-Mo alloys and only well-annealed samples can be considered as compounds. This might be the origin of the various different experimental results published on the R(Fe,Mo)$_{12}$ series.

Magnetization measurements on fine TbFe$_{10}$Mo$_2$ powders, loaded loosely into the sample holder, in fields up to 35 T show no indication of the decoupling of the ferrimagnetically coupled Tb- and Fe-sublattice moments. This suggests that the field strength of 35 T is not high enough to decouple Tb and Fe moments in TbFe$_{10}$Mo$_2$.

F. DyFe$_{10}$Mo$_2$

Dy-containing ThMn$_{12}$ type of compounds have been reported to show more than one spin reorientation.[6–8] A complex variation of the EMD with temperature is proposed for DyFe$_{11}$Ti and DyFe$_{10}$Cr$_2$ between 4.2 and 300 K.[7,43] In the present study, only one spin-reorientation transition has been detected for DyFe$_{10}$Mo$_2$ at 137 K both in the temperature dependence of the ac susceptibility (Fig. 12) and of the magnetization (Fig. 8). From the magnetization of magnetically aligned DyFe$_{10}$Mo$_2$ shown in Fig. 13 (see also the discussion in Sec. IV C), it is concluded that the EMD changes from the c axis at high temperature ($T > 137$ K) to a cone at low temperature ($T < 137$ K). The magnetization of fine DyFe$_{10}$Mo$_2$ powder, loaded loosely into the sample holder, was measured at 4.2 K in fields up to 35 T. At high fields, the magnetization exhibits a strong increase (Fig. 14) which corresponds to the departure of the Dy and Fe moments from the ferrimagnetic structure. From the magnetization behavior in the highest fields, a value for the intersublattice-molecular-field coefficient $n_{R\text{-}T}$ in DyFe$_{10}$Mo$_2$ can be estimated, which is listed in Table II together with the corresponding value for $J_{R\text{-}T}$.

G. HoFe$_{10}$Mo$_2$

The temperature dependence of the ac susceptibility (Fig. 5) and of the magnetization (Fig. 15) does not suggest any spin reorientation to occur in HoFe$_{10}$Mo$_2$. The magnetization of magnetically aligned HoFe$_{10}$Mo$_2$ at 4.2 K shows an anomalous increase around 2 T when the field is applied perpendicular to the alignment direction (Fig. 16). Such an anomaly has been found in other Ho-containing ThMn$_{12}$ compounds as well[8,44] and may be at-

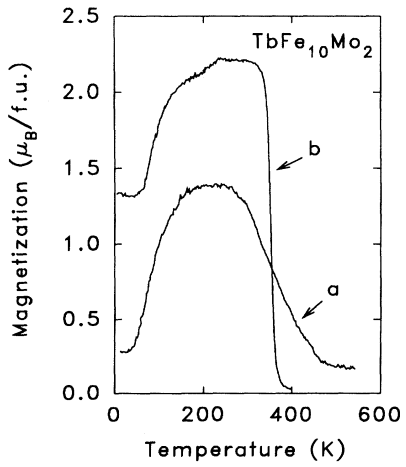

FIG. 11. Temperature dependence of the magnetization of a TbFe$_{10}$Mo$_2$ sample annealed at 1373 K for (a) 2 weeks and (b) another for 4 weeks. The applied field was 0.05 T.

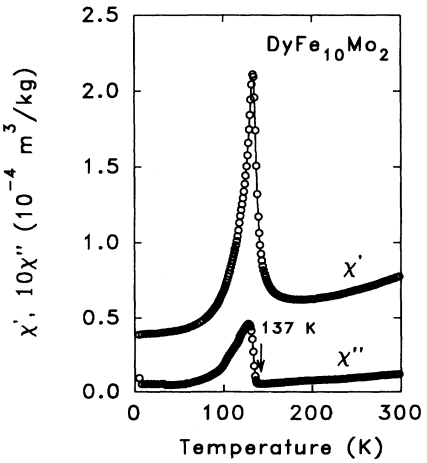

FIG. 12. Temperature dependence of the real (χ') and imaginary (χ'') components of the ac susceptibility of DyFe$_{10}$Mo$_2$. The applied ac field was 5×10^{-5} T and the frequency 1000 Hz.

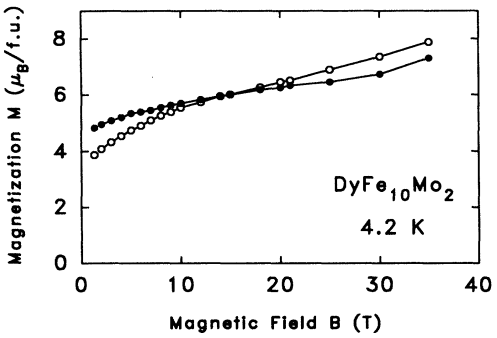

FIG. 13. High-field magnetization at 4.2 K of magnetically aligned $DyFe_{10}Mo_2$ with the field applied parallel (●) and perpendicular (○) to the alignment direction.

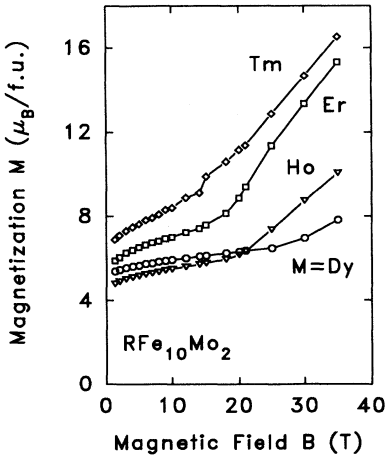

FIG. 14. High-field magnetization at 4.2 K of fine powder, loaded loosely into the sample holder, of $RFe_{10}Mo_2$ compounds with R = Dy, Ho, Er, and Tm.

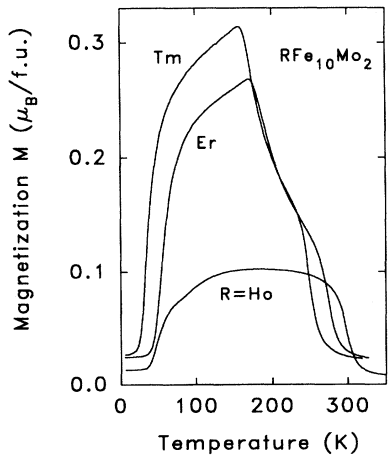

FIG. 15. Temperature dependence of the magnetization of $RFe_{10}Mo_2$ compounds with R = Ho, Er, and Tm. The applied field was 0.05 T.

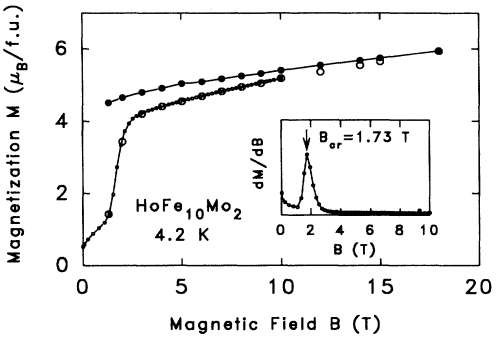

FIG. 16. High-field magnetization at 4.2 K of magnetically aligned $HoFe_{10}Mo_2$ with the field applied parallel (●) and perpendicular (○) to the alignment direction. The large and small dots represent the measurements obtained by employing "stepwise" and "continuous" field pulses. The inset shows dM/dB vs B for determining the critical field B_{cr} of the FOMP.

tributed to a FOMP-type transition. The value of the critical field of the FOMP can easily be determined from the maximum in the dM/dB versus B curve (inset of Fig. 16). The magnetization of fine $HoFe_{10}Mo_2$ powder, loaded loosely into the sample holder, was measured at 4.2 K in fields up to 35 T (Fig. 14). From the magnetization behavior in high fields, a value for the intersublattice-molecular-field coefficient $n_{R\text{-}T}$ in $HoFe_{10}Mo_2$ has been estimated, which is listed in Table II together with the corresponding value for $J_{R\text{-}T}$.

H. $ErFe_{10}Mo_2$

In the ac susceptibility of $ErFe_{10}Mo_2$ (Fig. 17) and also in the magnetization (Fig. 15), very pronounced anomalies are detected around 180 K. The peak at 289 K in the ac susceptibility corresponds to the Curie temperature. The magnetization behavior of magnetically aligned $ErFe_{10}Mo_2$ in fields parallel and perpendicular to the alignment direction indicates a change of the EMD between 4.2 and 300 K (Fig. 18). A FOMP type of transi-

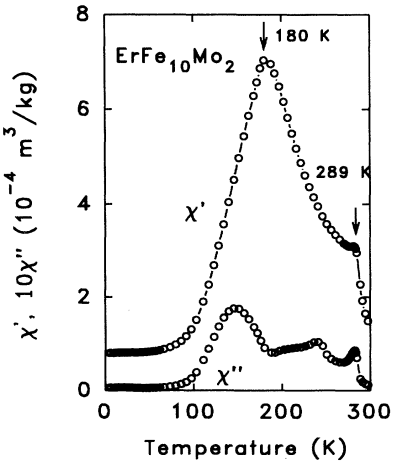

FIG. 17. Temperature dependence of the real (χ') and imaginary (χ'') components of the ac susceptibility of $ErFe_{10}Mo_2$. The applied ac field was 5×10^{-5} T and the frequency 1000 Hz.

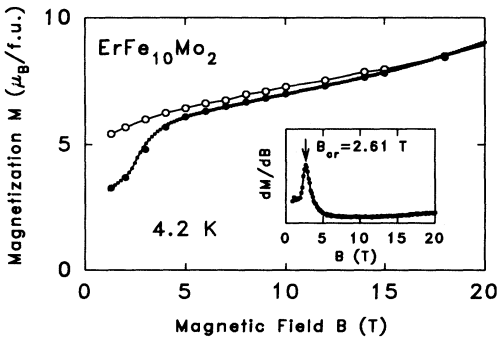

FIG. 18. High-field magnetization at 4.2 K of magnetically aligned $ErFe_{10}Mo_2$ with the field applied parallel (●) and perpendicular (○) to the alignment direction. The large and small dots represent measurements obtained by employing "stepwise" and "continuous" field pulses, respectively. The inset shows dM/dB vs B for determining the critical field B_{cr} of the FOMP.

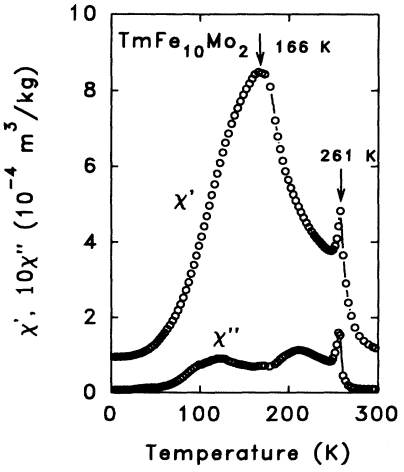

FIG. 19. Temperature dependence of the real (χ') and imaginary (χ'') components of the ac susceptibility of $TmFe_{10}Mo_2$. The applied ac field was 5×10^{-5} T and the frequency 1000 Hz.

tion is found in the magnetization of magnetically aligned $ErFe_{10}Mo_2$ when the field is applied parallel to the alignment direction. Considering these two observations, we conclude (see also the discussion in Sec. IV C) that a spin reorientation occurs in $ErFe_{10}Mo_2$ and that the EMD at 4.2 K has an angle larger than 45° with respect to the c axis. However, it is difficult to conclude whether the EMD at 4.2 K lies on a cone or in the basal plane. From a theoretical point of view, it would be hard to understand if the EMD would be in the basal plane. In terms of CEF calculations,[6–8,45] the net anisotropy of the Er ion in $ErFe_{10}Mo_2$ originates from the combined interactions of the CEF and the exchange field experienced by the Er ion. The exchange field is isotropic, whereas the CEF consists of three main contributions: the second-, fourth-, and sixth-order CEF terms. In the presence of a strong exchange field, the second-order CEF term $B_2^0O_2^0$, where $B_2^0<0$, shows no extreme (neither a maximum nor a minimum) as a function of the angle between the c axis and the magnetization, leading to an EMD parallel to the c axis. The fourth-order CEF term $B_4^0O_4^0$, where $B_4^0<0$, shows a minimum at 0°, leading to an EMD parallel to the c axis. The sixth-order CEF term $B_6^0O_6^0$, where $B_6^0>0$, shows a minimum at 30°, leading to an EMD tilted 30° with respect to the c axis. The values of B_2^0, B_4^0, and B_6^0 were estimated from Ref. [8]. In addition, the higher-order CEF terms change faster with temperature. The actual EMD depends on the competition between these CEF terms as they vary with temperature. In the case of $ErFe_{10}Mo_2$, the sixth-order CEF term is suggested to be dominant at 4.2 K, which leads to an EMD tilt of nearly 30° with respect to the c axis. This is smaller than derived from the experiments. However, from this discussion, even though it is qualitative, it is clear that at 4.2 K the EMD in $ErFe_{10}Mo_2$ cannot be within the basal plane. It is worthwhile to note that without a detailed study of the magnetization on an $ErFe_{10}Mo_2$ single crystal, we are not able to provide an exact explanation for the spin reorientation detected in $ErFe_{10}Mo_2$. The magnetization of fine $ErFe_{10}Mo_2$ powder, loaded loosely into the sample holder, in fields up to the 35 T, is shown in Fig. 14. From the magnetization behavior in high fields, a value for the intersublattice-molecular-field coefficient $n_{R\text{-}T}$ in $ErFe_{10}Mo_2$ has been estimated, which is listed in Table II together with the corresponding value for $J_{R\text{-}T}$.

I. $TmFe_{10}Mo_2$

For $TmFe_{10}Mo_2$, similar to $ErFe_{10}Mo_2$, a pronounced anomaly is detected at about 166 K both in the temperature dependence of the ac susceptibility (Fig. 19) and of the magnetization (Fig. 15). Since the Curie temperature of $TmFe_{10}Mo_2$ (261 K) is below room temperature, magnetic alignment at room temperature is not effective and magnetization measurements on magnetically aligned samples give no information concerning the change of the EMD. Since the three CEF parameters B_2^0, B_4^0, and B_6^0, estimated from the study of $TmFe_{11}Ti$,[8] are all negative in sign, the second-, fourth-, and sixth-order CEF terms contribute a c-axial anisotropy to the net anisotropy. No spin-reorientation transition is expected in $TmFe_{10}Mo_2$. However, the experimental result is very similar to that on $ErFe_{10}Mo_2$, suggesting that the CEF experienced by a Tm^{3+} ion in $TmFe_{10}Mo_2$ may be different from that in $TmFe_{11}Ti$. The experimental suggests that the EMD in $TmFe_{10}Mo_2$ changes from the c axis above 166 K to a cone configuration below 166 K. The magnetization of fine $TmFe_{10}Mo_2$ powder, loaded loosely into the sample holder, was measured at 4.2 K with fields up to 35 T (Fig. 14). From the magnetization behavior in high fields, a value for the intersublattice-molecular-field coefficient $n_{R\text{-}T}$ in $TmFe_{10}Mo_2$ has been estimated, which is listed in Table II together with the corresponding value for $J_{R\text{-}T}$.

V. SUMMARY AND CONCLUSIONS

In the present paper, a systematic study of the magnetic properties of tetragonal $ThMn_{12}$-type $RFe_{10}Mo_2$ compounds has been presented. Spin reorientations have

been detected in the compounds with R=Nd, Dy, Er, and Tm. In the compounds with R=Pr, Ho, and Er, a FOMP-like transition is found at low temperatures. The anomalous increase of magnetization of $SmFe_{10}Mo_2$ at low temperatures is suggested to be a fast continuous rotation of the magnetic moment under the action of an external field, rather than a FOMP type of transition. A diagram representing the variation of the EMD with temperature for each $RFe_{10}Mo_2$ compound studied is presented in Fig. 20.

Compared to other $R(Fe,M)_{12}$ compounds, the $RFe_{10}Mo_2$ series is anomalous in several respects: First of all, in order to stabilize $RFe_{10}Mo_2$ compounds, annealing at a high temperature for a long time is necessary. The Curie temperatures and the magnetization values of $RFe_{10}Mo_2$ are lower than for the other $RFe_{10}M_2$ (M=V,Cr,W, . . .) compounds. The anisotropy field of $YFe_{10}Mo_2$ is only detectable below 150 K, far below the Curie temperature. $PrFe_{10}Mo_2$ is the only Pr-containing $ThMn_{12}$ type of compound that shows a FOMP type of transition at low temperature. $TbFe_{10}Mo_2$ is the only Tb-containing $ThMn_{12}$ type of compound that does not show a spin reorientation. $ErFe_{10}Mo_2$ is the only Er-containing $ThMn_{12}$ type of compound that shows a FOMP-like transition when the field is applied parallel to the alignment direction. $TmFe_{10}Mo_2$ is the only Tm-containing $ThMn_{12}$ type of compound that exhibits a spin reorientation.

From the values of $J_{R\text{-}T}$ listed in Table II, it follows that the R-T coupling strength in ferrimagnetic $RFe_{10}Mo_2$ compounds has a clear tendency to decrease with increasing atomic number Z of the R ions. Belorizky *et al.*[22] have explained this reduction in terms of the strong decrease of the radius of the $4f$ shell with increasing Z which is accompanied by a reduced $4f$-$5d$ interaction. From atomic calculations by Brooks *et al.*[46–48] and by Li, Li, and Coey,[49] it was derived that the values of the exchange integral $J_{4f\text{-}5d}$ decreases from Ce to Yb. An extension of the free-powder magnetization measurements to higher fields (38 T), and an analysis of the occurring deviation from exact linear behavior of the magnetization in the high-field regime are presently being carried out.[33]

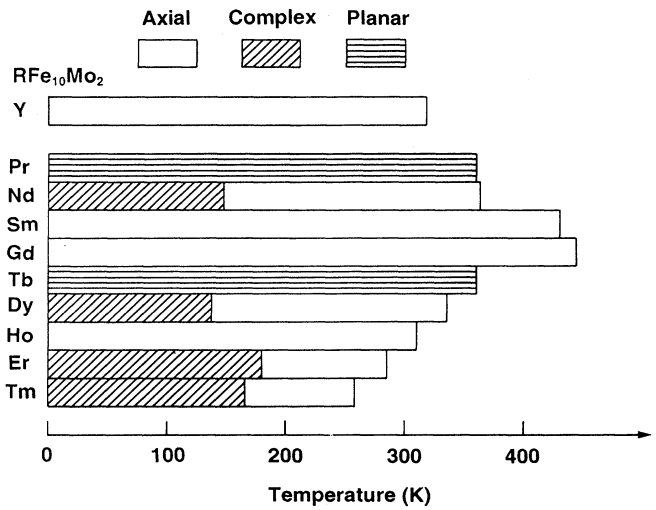

FIG. 20. Magnetic-anisotropy diagram for the $RFe_{10}Mo_2$ compounds.

ACKNOWLEDGMENTS

This work was supported by the Fonds zur Förderung der Wisenschaftlichen Forschung of Austria under the project Nos. S5604, S5605, and 7620. The high-field measurements in the Amsterdam High Field Installation have been carried out within the scientific exchange program between China and the Netherlands. The authors thank Lu Ping for x-ray-diffraction analysis and Dr. A. Kerr for critically reading the manuscript.

[1]F. R. de Boer, Huang Ying-kai, D. B. de Mooij, and K. H. J. Buschow, J. Less-Common Met. **135**, 199 (1987).
[2]B. D. de Mooij and K. H. J. Buschow, Philips J. Res. **42**, 246 (1987).
[3]D. B. de Mooij and K. H. J. Buschow, J. Less-Common Met. **136**, 207 (1988).
[4]R. Verhoef, F. R. de Boer, Zhang Zhi-dong, and K. H. J. Buschow, J. Magn. Magn. Mater. **75**, 319 (1988).
[5]K. H. J. Buschow, J. Magn. Magn. Mater. **100**, 79 (1991).
[6]Bo-Ping Hu, Hong-Shuo Li, J. P. Gavigan, and J. M. D. Coey, J. Phys. Condens. Matter **1**, 755 (1988).
[7]Bo-Ping Hu, Hong-Shuo Li, J. M. D. Coey, and J. P. Gavigan, Phys. Rev. B **41**, 2221 (1990).
[8]X. C. Kou, T. S. Zhao, R. Grossinger, H. R. Kirchmayr, X. Li, and F. R. de Boer, Phys. Rev. B **47**, 3231 (1993).
[9]O. Moze, L. Pareti, M. Solzi, and W. I. F. David, Solid State Commun. **66**, 465 (1988).
[10]Lu Ping and E. Gratz (unpublished).
[11]J. Ding and M. Rosenberg, J. Magn. Magn. Mater. **83**, 257 (1990).
[12]L. Schultz, K. Schnitzke, and J. Wecker, J. Magn. Magn. Mater. **83**, 254 (1990).
[13]C. Christides, A. Kostikas, X. C. Kou, and R. Grössinger, J. Phys. Condens. Matter **5**, 8611 (1993).
[14]C. Christides, A. Kostikas, G. Zouganelis, V. Psyharis, X. C. Kou, and R. Grössinger, Phys. Rev. B **47**, 11 220 (1993).
[15]Hong Sun, M. Akayama, K. Tatami, and H. Fujii, Physica B **183**, 33 (1993).
[16]Hong Sun, M. Akayama, and H. Fujii, Phys. Status Solidi A **140**, K107 (1993).
[17]X. C. Kou, E. H. C. P. Sinnecker, R. Grössinger, G. Wiesinger, T. Zhao, J. P. Liu, and F. R. de Boer, J. Magn. Magn. Mater. (to be published).
[18]I. Kleinschroth (unpublished).
[19]R. Gersdorf, F. R. de Boer, J. C. Wolfrat, F. A. Muller, and L. W. Roeland, in *High Field Magnetism*, edited by M. Date (North-Holland, Amsterdam, 1983), p. 277.
[20]X. C. Kou, C. Christides, R. Grössinger, H. R. Kirchmayr, and A. Kostikas, J. Magn. Magn. Mater. **104-107**, 1341 (1992).

[21]X. C. Kou and R. Grössinger, J. Magn. Magn. Mater. **95**, 184 (1991).
[22]E. Belorizky, M. A. Fremy, J. P. Gavigan, D. Givord, and H. S. Li, J. Appl. Phys. **61**, 3971 (1987).
[23]N. H. Duc, T. D. Hien, D. Givord, J. J. M. Franse, and F. R. de Boer, J. Magn. Magn. Mater. **124**, 305 (1993).
[24]M. Loewenhaupt, M. Prager, A. P. Murani, and H. E. Hoenig, J. Magn. Magn. Mater. **76-77**, 408 (1988); M. Loewenhaupt, I. Sosnowska, and B. Fiick, Phys. Rev. B **42**, 3866 (1990); M. Loewenhaupt, I. Sonsnowska, A. Taylor, and R. Osborn, J. Appl. Phys. **69**, 5593 (1991); **70**, 5967 (1991).
[25]A. E. Clark and E. J. Callen, J. Appl. Phys. **39**, 5972 (1968).
[26]R. Grössinger and G. Hilscher, J. Phys. (Paris) Colloq. **40**, C5-202 (1979).
[27]R. Grössinger and J. Liedl, IEEE Trans. Magn. **MAG-17**, 3005 (1981).
[28]R. Verhoef, R. J. Radwanski, and J. J. M. Franse, J. Magn. Magn. Mater **89**, 176 (1990).
[29]J. P. Liu, F. R. de Boer, P. F. de Châtel, R. Coehoorn, and K. H. J. Buschow, J. Magn. Magn. Mater. **132**, 159 (1994).
[30]R. J. Radwanski and J. J. M. Franse, J. Magn. Magn. Mater. **74**, 43 (1988).
[31]F. R. de Boer and K. H. J. Buschow, Physica B **177**, 199 (1992).
[32]Z. G. Zhao, Ph.D. thesis, University of Amsterdam, 1994.
[33]Z. G. Zhao, J. P. Liu, X. C. Kou, and F. R. de Boer (unpublished).
[34]R. Ballou, J. Deportes, and J. Lemaire, J. Magn. Magn. Mater. **70**, 306 (1987).
[35]T. S. Zhao, H. M. Jin, G. H. Guo, X. F. Han, and H. Chen, Phys. Rev. B **43**, 8593 (1991).
[36]T. S. Zhao, H. M. Jin, R. Grössinger, X. C. Kou, and H. R. Kirchmayr, J. Appl. Phys. **70**, 6134 (1991).
[37]X. C. Kou, R. Grössinger, H. Müller, and K. H. J. Buschow, J. Magn. Magn. Mater. **101**, 349 (1991).
[38]S. Hirosawa, Y. Matsuura, H. Yamamoto, S. Fujimura, M. Sagawa, and H. Yamauchi, J. Appl. Phys. **59**, 873 (1986).
[39]X. C. Kou and R. Grössinger (unpublished).
[40]D. Givord and R. Lemaire, IEEE Trans. Magn. **MAG-10**, 109 (1974).
[41]G. Asti, in *Ferromagnetic Materials,* edited by K. H. J. Buschow and E. P. Wohlfarth (North-Holland, Amsterdam, 1990), Vol. 5, p. 397.
[42]T. Kaneko, M. Yamada, K. Ohashi, T. Tawara, R. Osugi, H. Yoshida, G. Kido, and Y. Nakagawa, *Proceedings of the 10th International Workshop on Rare Earth Magnets and Their Applications,* Kyoto, Japan (The Society of Non-traditional Metallurgy, Kyoto, Japan, 1989), p. 191.
[43]Yang Fuming, Q. A. Li, R. W. Zhao, J. P. Kuang, F. R. de Boer, K. V. Rao, G. Nicolaides, and K. H. J. Buschow, J. Alloys Compounds **177**, 93 (1991).
[44]J. P. Liu, Ph.D. thesis, University of Amsterdam, 1994.
[45]M. Yamada, H. Kato, H. Yamamoto, and Y. Nakagawa, Phys. Rev. B **38**, 620 (1988).
[46]M. S. S. Brooks, O. Eriksson, and B. Johansson, J. Phys. Condens. Matter **1**, 5861 (1989).
[47]M. S. S. Brooks, L. Nordström, and B. Johansson, J. Phys. Condens. Matter **3**, 2357 (1991); Physica B **172**, 95 (1991); J. Appl. Phys. **69**, 5683 (1991).
[48]M. S. S. Brooks, T. Gasche, S. Auluck, L. Nordström, L. Severin, J. Trygg, and B. Johansson, J. Appl. Phys. **70**, 5972 (1991); J. Magn. Magn. Mater. **104-107**, 1381 (1992).
[49]H.-S. Li, Y. P. Li, and J. M. D. Coey, J. Phys. Condens. Matter **3**, 7277 (1991); J. Magn. Magn. Mater. **104-107**, 1444 (1992).